Ultrafast dynamics of excitons in tetracene single crystals

Zephania Birech, Markus Schwoerer, Teresa Schmeiler, Jens Pflaum, and Heinrich Schwoerer

Articles you may be interested in

Photoisomerization among ring-open merocyanines. I. Reaction dynamics and wave-packet oscillations induced by tunable femtosecond pulses
J. Chem. Phys. **140**, 224310 (2014); 10.1063/1.4881258

Impact of intramolecular twisting and exciton migration on emission efficiency of multifunctional fluorene-benzothiadiazole-carbazole compounds
J. Chem. Phys. **134**, 204508 (2011); 10.1063/1.3594047

Excited state dynamics in solid and monomeric tetracene: The roles of superradiance and exciton fission
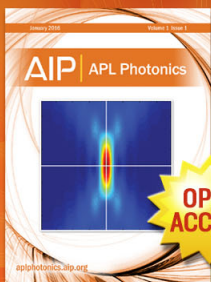J. Chem. Phys. **133**, 144506 (2010); 10.1063/1.3495764

Ultrafast dynamics of excitons in delafossite CuScO 2 thin films
Appl. Phys. Lett. **96**, 211904 (2010); 10.1063/1.3436548

Femtosecond studies of exciton dynamics in a novel main chain chiral conjugated poly(arylenevinylene)
J. Chem. Phys. **106**, 3710 (1997); 10.1063/1.473423

Ultrafast dynamics of excitons in tetracene single crystals

Zephania Birech,[1,a)] Markus Schwoerer,[2] Teresa Schmeiler,[3] Jens Pflaum,[3] and Heinrich Schwoerer[1,b)]

[1]*Laser Research Institute, Stellenbosch University, Stellenbosch 7600, South Africa*
[2]*Department of Physics, University of Bayreuth, Bayreuth, Germany*
[3]*Experimental Physics VI, University of Würzburg and Bavarian Center for Applied Energy Research, Würzburg, Germany*

Ultrafast exciton dynamics in free standing 200 nm thin tetracene single crystals were studied at room temperature by femtosecond transient absorption spectroscopy in the visible spectral range. The complex spectrally overlapping transient absorption traces of single crystals were systematically deconvoluted. From this, the ultrafast dynamics of the ground, excited, and transition states were identified including singlet exciton fission into two triplet excitons. Fission is generated through both, direct fission of higher singlet states S_n on a sub-picosecond timescale, and thermally activated fission of the singlet exciton S_1 on a 40 ps timescale. The high energy Davydov component of the S_1 exciton is proposed to undergo fission on a sub-picoseconds timescale. At high density of triplet excitons their mutual annihilation (triplet-triplet annihilation) occurs on a <10 ps timescale. © 2014 AIP Publishing LLC. [http://dx.doi.org/10.1063/1.4867696]

I. INTRODUCTION

For more than half a century polyacene crystals, such as naphthalene, anthracene, tetracene, and pentacene have been prototypes for the investigation of the basic electrical and optical properties and processes of many organic semiconductors.[1,2] Within the past decade special emphasis was given to crystalline tetracene (Tc), which has been used as the active semiconductor in developing novel organic electronic devices including ambipolar organic light emitting transistors (OLETs),[3] organic field-effect transistors (OFETs),[4–7] and organic solar cells (OSCs).[8,9] In order to understand the fundamental electronic properties and their dynamics upon photo-excitation steady state absorption,[10–12] emission,[10,13–16] photoemission,[17] and transient absorption[18–25] spectroscopy studies on both Tc crystals and Tc polycrystalline thin films have been used.

The relevant electronic excitations in polyacene crystals are the lowest singlet (S_1) and triplet (T_1) Frenkel excitons below the electronic transport gap and charge transfer excitons with total spin quantum numbers **S** = 0 and **S** = 1 for singlet and triplet excitons, respectively. Both, singlet and triplet excitons are excitations of the crystal unit cell containing two translationally invariant molecules. Singlet and triplet excitons have the ability to diffuse through the crystal during their lifetime, thereby transporting their excitation energy. The radiative $T_1 \to S_0$ transition to the S_0 ground state is spin forbidden. Therefore, lifetimes of T_1 in all polyacene crystals are orders of magnitude longer compared to lifetimes of S_1. Due to the van der Waals interaction of the two translationally invariant molecules in the unit cell all these excitons exhibit Davydov splitting (DS).[10,12,26] The DS for the 0-0 vibra-

tional band of the optically allowed transition $S_1 \leftarrow S_0$ with polarization normal to the *ab* plane of the Tc crystal is about 0.08 eV.[10,12]

A further unique optical property generating interest in the development of photovoltaic cells is singlet exciton fission. Singlet fission in tetracene is a radiationless process, in which one singlet exciton on a tetracene dimer decays via an intermediate multiexciton state into two triplet excitons (Fig. 1), which subsequently diffuse apart.[27,28] Singlet exciton fission (SEF) is spin allowed since the two resulting triplet excitons initially emerged from the same singlet state.[27,29–31] SEF is known to exist in Tc crystals as a very fast process since decades.[27,28,32] It has also been observed in crystalline anthracene,[33] polycrystalline Tc[18–21] and pentacene thin films, and single crystals.[22,28,33–35] Covalently linked Tc dimers have also exhibited SEF but with very low triplet exciton yield.[36] A condition for the occurrence of SEF is that the energy of the first excited singlet state must be at least twice that of the first excited triplet state, i.e., $E(S_1) \gtrsim 2E(T_1)$, at least at temperature $T = 0$ K.[27] This condition is readily met in pentacene but for Tc the process should be thermally activated since $E(S_1) - 2E(T_1) \approx -0.2$ eV.[22,34,37] However, recent time resolved two-photon photon-emission experiments on tetracene crystal surfaces suggest an entropy driven singlet fission process through a multiexciton state: $S_1 \to ME \to 2\,T_1$.[17]

An application of singlet exciton fission relies on the superior diffusion length of the generated triplet excitons and the potential to surpass the Shockley-Queisser limit for single junction photovoltaic cells by a factor of 1.5 if the excess solar energy photons above the band gap are converted into more than one electron-hole pair per photon.[38–41] This potential has led to an increased research focus on how SEF occurs in Tc[18–22,27,37] and pentacene (Pc).[23,29,42] The opposite process, exciton fusion of the two triplet excitons forming a

---

a)Present address: Department of Physics, University of Nairobi, Nairobi, Kenya.
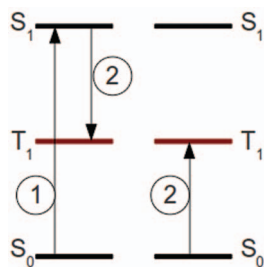b)heso@sun.ac.za

140, 114501-1

FIG. 1. Singlet fission schematic. (1) An S_1 exciton state (left) is initially excited in the tetracene crystal. (2) This exciton then shares its energy with an adjacent ground state (right) and in the process two triplet excitons T_1 are created per absorbed photon.[27]

singlet exciton can also occur. The formed singlet then undergoes radiative relaxation to the ground state, referred to as delayed fluorescence, the specific magnetic field dependence of which acts as perfect proof of intermediate formation of triplet excitons.[18,27,28] Tc is an ideal material for femtosecond time resolved studies of the interaction between singlet and triplet excitons, since unlike pentacene, once the triplets have been formed they can interact leading to their annihilation and reforming back singlet excitons.

The main focus of our experimental work to be presented in this paper was the study of the ultrafast dynamics of singlet and triplet excitons, including SEF, in free standing Tc single crystals by femtosecond transient absorption spectroscopy. The transient absorption spectra were systematically deconvoluted in order to identify excited and transition states, and to follow their evolution on a femtosecond to nanosecond time scale.

II. EXPERIMENTAL

Tc single crystals were grown by horizontal physical vapor growth[43] under an inert gas atmosphere of 99.9999% pure nitrogen. The material's sublimation temperature amounts to 200 °C at standard pressure. Platelets with extended (ab)-facets and lateral dimensions of several millimeters up to 1 cm and thicknesses between 100 μm and 500 μm have been obtained. Figure 2(a) shows three examples of about 500 μm thickness. Furthermore, the high absorptivity of polyacene crystals (of the order of 10^5 cm^{-1} at the maximum of their $S_1 \leftarrow S_0$ absorption) requires very thin specimen for trans-
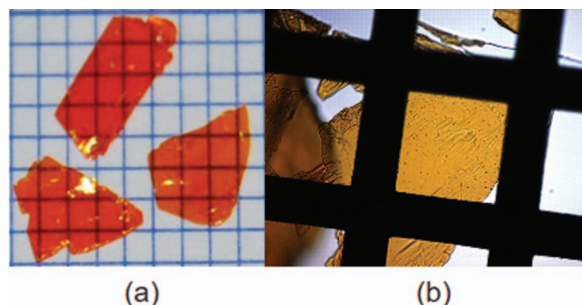

FIG. 2. Images of (a) Tc as grown crystal platelets of thickness $\approx$500 μm on a blue square grid with 1 mm divisions and (b) a 300 nm thick Tc single crystal supported on a copper wire mesh with squares of dimensions 150 μm.

mission spectroscopy measurements. Therefore, the as grown crystals were cleaved using a microtome and were supported on a TEM copper wire grid with squares of lateral dimension 150 μm as shown in Figure 2(b).

Both steady state and transient absorption (TA) measurements have been carried out under ambient condition at room temperature on the same experimental setup which closely follows the design described in detail in Ref. 44. The light source for absorption measurements was a single filament femtosecond white light continuum (WLC) generated by focusing a femtosecond laser pulse (ClarkMXR, CPA2101) onto a 3 mm thick calcium fluoride (CaF$_2$) crystal (laser pulse duration $\approx$150 fs, wavelength 775 nm, repetition rate: 1 kHz). The CaF$_2$ crystal was continuously moved to prevent photo damage and to ensure stability of the femtosecond white light continuum. The generated WLC spectrum extended from 340 nm to the near infrared (NIR). The beam transmitted through the sample was dispersed in a spectrometer (Andor SR163) and detected at a 1 kHz rate with a 1024 pixel photodiode array. Samples in solution were pumped through a 1 mm path length quartz cuvette.

For the transient absorption measurements, the sample was excited by a pump laser pulse and the absorption of the white light continuum was detected at a variable delay time. The pump laser pulses are either centered around 387 nm (fundamental laser pulse frequency doubled in a beta-barium borate BBO crystal) or tunable between 450 nm and 700 nm, generated in a non-collinear parametric amplifier delivering 30 fs pulses. Pump intensities below 4 GW/cm^2 were applied in order to avoid nonlinear excitation, and to assure an appreciable signal-to-noise ratio. This corresponds to a pump fluence in the order of 100 μJ/cm^2, which might induce a nonlinear singlet deexcitation in the crystal, see below. The pump beam was chopped at the rate of 500 Hz before overlapping with the probe beam at the sample position, resulting in alternating absorption spectra of excited (pumped) and not excited (unpumped) sample. Changes in the sample's optical density ($\triangle OD(\lambda, t)$) were then calculated. The time delay between the probe and the pump pulses was varied by moving a retroreflector on a computer controlled delay line in the optical beam path of the pump pulse. The temporal resolution of the setup was $\approx$200 fs, mainly governed by the duration and accuracy of chirp correction on the WLC probe pulses.[44] A Glan-Taylor calcite polarizer and an achromatic half wave-plate in the laser beam path allow polarization control of the white light. For the Tc molecules in solution a magic angle of 54.7° was set between the probe and the pump beams in order to eliminate effects due to re-orientation of transition dipole moments.[45]

III. RESULTS AND DISCUSSION

A. Steady state absorption and Davydov splitting

Figure 3(a) displays the steady state absorption spectrum (SSA) of Tc in toluene (concentration 4.7×10^{-6} moles/cm^3). It reveals a vibronic progression of the $S_1 \leftarrow S_0$ transition, arising from the collective $C = C/C - C$ stretching mode[46–48] with energy of 0.17 eV. The center wavelengths of the
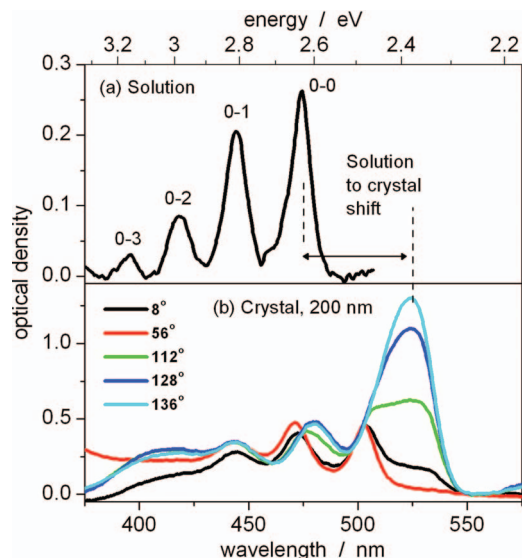
FIG. 3. Steady state absorption spectrum of Tc in solution (a) and the 200 nm thick single crystal (b). The spectra marked the $S_1^v \leftarrow S_0$ transition (v = vibrational band). The solution to crystal shift is indicated. The crystal spectra were measured at an interval of 8° rotation of an achromatic half wave-plate which varied the polarization of the exciting optical field. Spectra at some selected polarization angles are displayed in (b).

0-0, 0-1, 0-2, and 0-3 vibrational bands are displayed in Table I and agree well with published data.

Absorption spectra of the 200 nm thick single crystal are displayed in Figure 3(b) for different angles of polarization of the exciting optical field within the ab-plane of the crystal (see below). The solution to crystal redshift arises due to aggregate formation accompanied by non-resonant interactions of excited and neighboring ground state molecules.[2,26] Its value ranges from 0.15 eV to 0.23 eV in the 0-0 vibrational band, depending on polarization, as shown in Table I.

The polarization dependence of the crystal spectra reveals the Davydov splitting (DS) which is a consequence of overlap of the wavefunctions of the two translational invariant molecules in the unit cell forming two dimer wavefunctions with orthogonally polarized optical transitions. These two bands, the high and the low energy Davydov components in the S_1 state, are excitable with optical fields polarized perpendicular and parallel to b axis of Tc, respectively.[26] This corresponds to the spectra labeled 56° (red) and 136° (cyan) in Figure 3(b) giving minimum and maximum absorbance values in the 0-0 vibrational peak, respectively (the experimental

TABLE I. Table giving the center wavelengths for the vibrational bands of the $S_1 \leftarrow S_0$ transition in both, Tc in solution and Tc single crystals, Davydov splittings (DS) and solution to crystal (SC) shift energy values.

Sample	Pol.	(0-0)	(0-1)	(0-2)	(0-3)
Solution	(nm)	474	444	418	395
Crystal 200 nm	⊥ b (nm)	503	472	444	
	∥ b (nm)	519	477	443	
DS	(eV)	0.08	0.03	0.01	
SC shift	⊥ b (eV)	0.15	0.17	0.17	
SC shift	∥ b (eV)	0.23	0.19	0.17	

angle difference is not exactly 90° due to the large step size used). The obtained DS energy of 0.08 eV from the lowest vibrational band in S_1 compares well with those reported by Tavazzi *et al.*[10] and Yamagata *et al.*[12] implying that our samples do not get significantly modified during microtoming and subsequent handling and storage.

B. Femtosecond transient absorption spectroscopy

Femtosecond transient absorption (TA) was employed to study dynamics of photogenerated states in Tc in solution as well as in Tc single crystals.

1. Tetracene in toluene

Figure 4 displays TA spectra of Tc in toluene between 390 nm (3.2 eV) and 570 nm (2.2 eV) for different times after photo-excitation with a 150 fs pump pulse centered at $\lambda = 387$ nm and a rescaled steady state absorption spectrum for reference. The TA spectra ($\Delta OD(\lambda, t)$) display changes of absorption with reference to steady state absorption.

The observed spectra are positive throughout the spectral window, indicating a dominating broad band excited state absorption (ESA). Comparison with the steady state absorption (SSA) reveals that the minima at 474 nm and 444 nm are caused by the depopulation of Tc ground state (ground state bleach). A similar spectrum was reported by Burdett *et al.*[18] The insert displays the TA spectrum after 10 ns: the intense ESA around 418 nm (2.97 eV) has decayed, signifying a transfer of excitation energy to low energy states, most likely lying outside our spectral window or being of dark state character. The radiative lifetime of S_1 in Tc solution was previously reported to be 23 ns.[36] The dominant broad positive signal detected within the temporal region of our experiment was therefore due to $S_n \leftarrow S_1$ transitions.

A notable feature is a small maximum at 465 nm (2.67 eV) appearing on a 20 ps time scale, which is even more pronounced after 10 ns (see inset of Figure 4) indicating
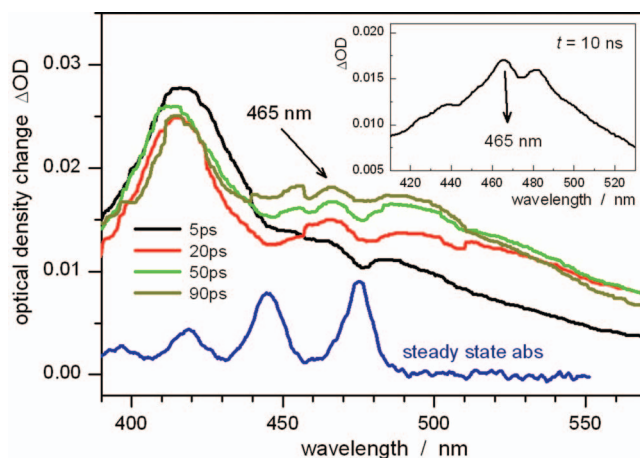

FIG. 4. Femtosecond TA spectra traces of Tc in solution at different times after excitation. The signal is dominated by a broad positive ESA contribution. Dips on this signal represent ground state bleaching (GSB) signals as they are at exactly same positions as those of the steady state absorption (SSA). A small maximum is noticed at 465 nm 20 ps after excitation and is more prominent in the 10 ns trace displayed in the inset.
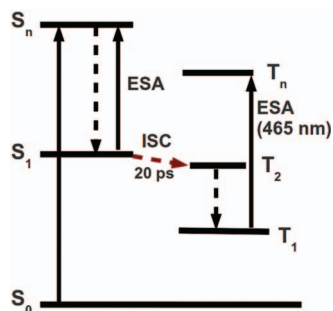
FIG. 5. Proposed model to explain the observed signal attributed to the $T_n \leftarrow T_1$ transitions in the monomer 20 ps after excitation. The energy of S_1 was higher than T_2 which then made ultrafast inter-system crossing more probable competing with internal conversion. The broad positive peak must be caused by $S_n \leftarrow S_1$ transitions as shown.

its long living nature. This maximum was situated where a triplet-triplet absorption ($T_n \leftarrow T_1$) was identified before by Bensasson and Land *et al.*[49] through flash photolysis experiments on Tc (termed naphtacene in Ref. [49]) in benzene. A possible explanation of this surprisingly fast triplet state population is dimerization or aggregation of Tc molecules which then facilitate singlet exciton fission (SEF). Covalently linked Tc dimers have previously displayed exciton fission but with very low yields.[36] If this were so, then the positions of the vibrational peaks in the SSA spectrum were expected to be red-shifted relative to those established in literature.[12,26,36,50,51] This however, was not observed.

A more likely explanation is an excited triplet state T_2 close to the first excited singlet state S_1, which might facilitate the occurrence of an ultrafast intersystem crossing (ISC) into the triplet manifold. The observed signal at 465 nm is thus ascribed to either $T_n \leftarrow T_1$ transitions or $T_n \leftarrow T_2$ transitions assuming a radiative life time longer than our experimentally accessible temporal window, while the broad ESA signal (400–600 nm) was due to $S_n \leftarrow S_1$ transitions (see Figure 5). Burdett *et al.* have identified a triplet state with a similar spectral feature at a delay of 20 ns.[18]

2. Tetracene single crystals, 387 nm and 530 nm excitation

Figure 6 displays the changes in optical density ($\Delta OD(\lambda, t)$) of the 200 nm thick single crystal as function of probe pulse wavelength (vertical axis) and temporal delay (horizontal axis) after excitation with 387 nm, 150 fs laser pulses. Red/yellow areas indicate increased absorption (ESA), while blue areas represent decreased absorption (ground state bleach, GSB or stimulated emission, SE). Green indicates no absorption change compared to the steady state absorption spectrum. The probe pulse is polarized $\parallel b$ axis of the (ab) crystal facet. It is apparent that the different spectral components in the TA spectrum strongly overlap. Therefore, a suitable deconvolution procedure must be applied. We reproduce the TA spectra at every time step as a sum of Gaussian shaped spectral components

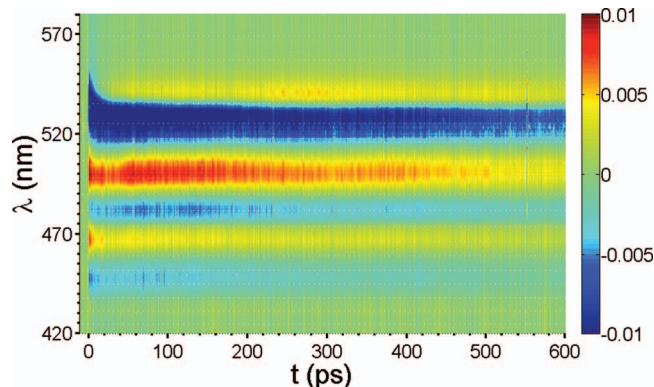$$G = \sum_i (A_i \times \exp[-((\lambda - \lambda_{i0})/\sigma_i)^2]).$$

FIG. 6. Map of the entire transient dynamics on the 200 nm thick crystal displayed on a two-dimensional array $\Delta OD(\lambda, t)$. The red/yellow bands represent wavelength regions of increased absorption (ESA) while blue bands represent regions of decreased absorption (GSB) or stimulated emission (SE).

with variable amplitude A_i, center wavelength λ_{i0}, and width σ_i. Figure 7 shows the signal at $t = 1$ ps and the result of a fitting procedure with nine Gaussian components. Apart from the amplitudes of these Gaussians, the parameters do not change significantly when the fit is applied on traces at different probe delays. The fit reproduces pretty well the general profile of the transient spectra.

Each spectral component of the deconvolution corresponds to a specific electronic transition, and is proportional to its respective oscillator strength. These transitions can be absorption of excited or transient states, ESA, which render positive ΔOD signals, stimulated emission, SE, probing fluorescence channels rendering negative ΔOD, or again negative ΔOD proportional to depleted Tc ground state, labelled ground state bleach GSB. The first step of the analysis is the comparison of transient and steady state spectra, see Figures 8(a) and 8(b). A positive signal in the steady state (ground state) absorption spectrum, appears as a negative signal in ΔOD just after excitation. The remaining positive transient signals must then be due to ESA, the remaining negative signals due to SE. The result of the deconvolution is given in
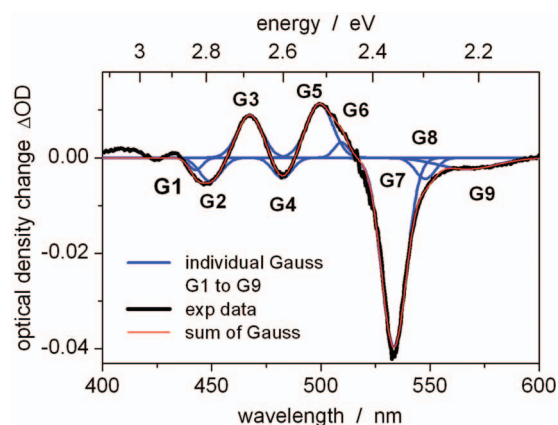

FIG. 7. TA spectrum trace of the 200 nm thick crystal at 1 ps after excitation deconvolved by fitting with a sum of Gaussians. The obtained fit reproduced the general profile pretty well. The positions of the Gaussian peaks G1 to G9 are also shown.
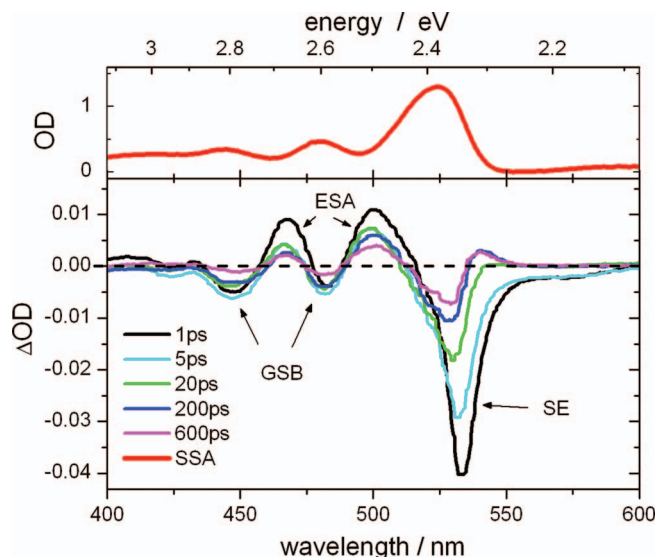
FIG. 8. The femtosecond TA signal traces from the 200 nm thick crystal pumped at 387 nm and probed with WLC polarized parallel to the b axis of the *ab* plane of the crystal unit cell. The signal consisted of GSB, ESA, and SE contributions. The GSB contributions at 444 nm, 478 nm, and 520 nm were located at the positions of the vibrational bands in steady state absorption (SSA) spectrum displayed in the upper panel. A short lived (10 ps) stimulated emission (SE) was observed at 533 nm. Long living excited state absorption (ESA) signals were observed at around 468 nm and 499 nm.

Table II with GSB signals identified, and SE and ESA still to be interpreted.

3. Excited state absorption and singlet exciton fission

Transient absorption spectra at various times are displayed in Figure 8, demonstrating dynamics on different time scales. We first focus on the dynamics and assignment of the ESA signals at 468 nm (2.65 eV, G3) and at 499 nm (2.49 eV, G5). Their temporal evolution is plotted in Figure 9, black data points. Both traces show an ultrafast rise and decay, followed by an increase on a 40 ps scale and a nanosecond final decay. For quantitative analysis, we model the traces with a sum of three exponential functions for the first decay (τ_1), the increase after the minimum (τ_2), and the final decay (τ_3). The initial ultrafast rise is assumed to be instantaneous within the experimental temporal resolution. The fit is convoluted with a Gaussian function reflecting the instrument response function with a width of 200 fs. The resulting traces are plotted as red lines in Fig. 8, the respective time constants and relative amplitudes are summarized in Table III. For interpretation we recall that the Tc singlet exciton life time at room temperature is about 145 ps[32] unlike triplet excitons
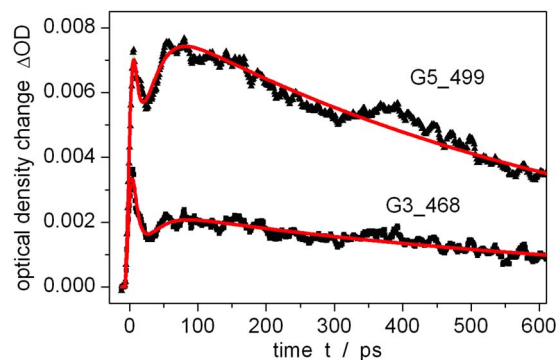

FIG. 9. The multi-exponential fit on the long decay dynamics (at around 468 nm and 499 nm) of the 200 nm thick crystals excited at 387 nm represented by the red line. The probe beam was polarized parallel to the b axis.

which live beyond ns.[18, 21, 22] The long life time τ_3, being several nanoseconds, therefore suggests that the signal originates from triplet absorption. Our ESA signal at 499 nm is therefore most likely due to $T_n \leftarrow T_1$ transitions. The signal at 468 nm displays similar temporal behavior and is attributed to a higher vibronic state of T_n. This assignment is supported by femtosecond TA studies on polycrystalline Tc thin films by Grumstrup *et al.* who ascribed the origin of an absorptive feature at 496 nm (which is close to 499 nm in our crystals) to the T_1 state.[21]

The temporal profiles of the triplet ESA signals are consistent with the model where a large population of singlet excitons is created in S_n states upon excitation at 387 nm (3.21 eV). These excitons relax on a sub-ps time scale via two channels, by internal conversion to S_1 and by direct Singlet Exciton Fission (SEF) via the multiexciton state $^1(T_1T_1)$ forming 2 triplet excitons $S_n \rightarrow {}^1(T_1T_1) \rightarrow 2T_1$ as schematically depicted in Figure 10. The ME state is an optically dark intermediate state resulting from triplet exciton twin with overall singlet spin multiplicity.[37, 52] These initial S_n relaxations are thought to account for the rapid rise in the ESA signals. If a dense population of T_1 excitons is created soon after relaxation, then triplet exciton-exciton annihilation is probable. The initial decay represented by τ_1 (see Table III) is then thought to represent this annihilation. This interpretation is supported by varying the excitation fluence: since annihilation requires the collision of two T_1 excitons, a higher triplet density accelerates annihilation.[2, 19] The life time of the initial ESA signal centered at 468 nm decreases from 4 ps to 2 ps upon increase in fluence from 240 μJ cm^{-2} to 410 μJ cm^{-2}, respectively, and its amplitude increases more than linear with the excitation fluence, see Figure 11, confirming the above assignment. A similar direct SEF process on a 300 fs time scale

TABLE II. The parameters used for the sum of Gaussian fits applied in Figure 7 for the 200 nm thick crystal. The Gaussians were grouped into GSB, ESA, and SE signals.

Gaussian	GSB			ESA			SE		
	G1	G2	G4	G3	G5	G6	G7	G8	G9
λ_0 (nm)	443	450	482	468	499	508	533	549	565
σ (nm)	7	11	12	14	13	8	15	9	35
A (a.u.)	−0.005	−0.008	−0.012	0.006	0.003	0.034	−0.003	−0.002	−0.002

TABLE III. The long decay dynamics exponential fit results for the crystals excited at center wavelengths (λ_{exc}) 387 nm and at 530 nm and crystals of thicknesses (x) 200 nm and 300 nm. A Gaussian response function of width 200 fs was used.

λ_{exc} (nm)	x (nm)	ESA (nm)	τ_1 (ps)	τ_2 (ps)	τ_3 (ps)	A_1	A_2	A_3
387	300	467	6	39	2000	0.089	0.02	−0.097
		496	5	40	3000	0.03	0.04	−0.31
	200	468	3	40	2000	0.07	0.006	−0.03
		499	5	37	1000	0.04	0.022	−0.057
530	300	468	8	73	1000	0.04	−0.03	−0.03
		498	14	72	1000	0.04	−0.05	−0.07

was recently proposed for Tc single crystals to explain a near infrared feature in a fs transmission experiment.[22] This result is also in agreement with what was reported by Burdett *et al.* in polycrystalline thin films.[19] However, in thin polycrystalline Tc films two polymorphs might co-exist leading to different time scales.[25]

The subsequent rise observed on a 40 ps timescale, see Figures 9 and 10, represents an increasing triplet yield due to thermally activated SEF $S_1 + \triangle E \rightarrow {}^1(T_1 T_1) \rightarrow 2T_1$. Comparable values of τ_1, τ_2, and τ_3, describing the ESA signal's temporal dynamics, are obtained for both the 200 nm and 300 nm thick crystals excited at 387 nm, see Table III. Thermally activated singlet fission has been reported to occur with a 37.5 ps time constant[21] in polycrystalline Tc and in 50 ps[22] in near infrared signatures of Tc single crystals. In singlet fluorescence measurements, probing the loss of S_1 forming S_0 (prompt fluorescence) and T_1 (delayed fluorescence), the process has been reported to occur on 100 ps[19,53] and 75 ps[16,21] timescales in polycrystalline thin films, if the pump fluence and thus the exciton density are sufficiently high to support singlet-singlet exciton annihilation processes. These time scales were approximately twice those obtained from TA studies which on the other hand probes absorption from T_1 states.

FIG. 11. The influence of increase in excitation fluence on the initial decay of ESA signal at 468 nm in the 300 nm thick crystal. The decay time constant changed from 4 ps to 2 ps with increase in excitation fluence from 240 μJ cm^{-2} to 410 μJ cm^{-2}, respectively. The amplitudes were also seen to increase.

The long living component might also originate from defect states. Defect states, with the most common being dislocations, vacancies, or guest molecules, are known to trap excitons.[2,15,18] The exact signatures of their influence in TA signals are debatable. The long living weak positive signal observed after 20 ps at around 540 nm (see Figure 8) might be attributed to absorption at defect's excited states.

The temporal profiles of GSB signals given by traces G4-482 and G1-443 are oppositely correlated with those of the ESA signals so far attributed to absorption from the T_1 state (traces G5-499 and G3-468) in Figure 12. This indicates that the bulk of the photogenerated excited states in Tc are indeed triplet excitons.

The stimulated emission signal represented by trace G7-533 displays two decay components, a fast one on a 8 ps timescale, see Figure 12, inset and Figure 10, and a slower component of about 200 ps. This SE signal is thought to emanate from the low energy Davydov state (2.39 eV, 520 nm in the steady state absorption). The fast component might be
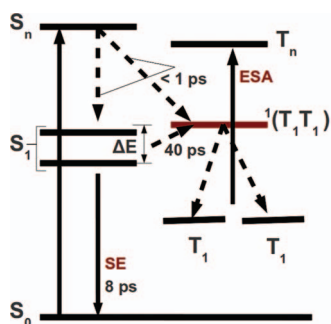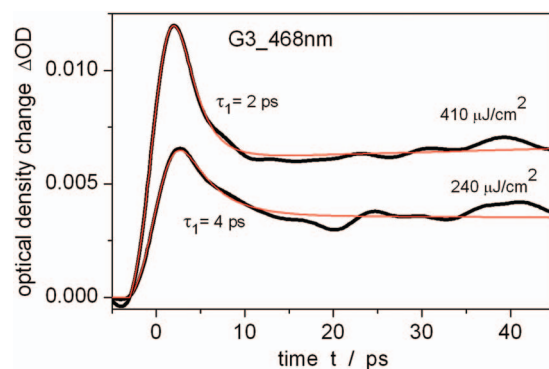

FIG. 10. A schematic showing the states involved in exciton fission with the two Davydov states, high energy and low energy, in S_1 shown. The high energy Davydov state is close to the multi-exciton (ME) state ${}^1(T_1 T_1)$. Exciton fission occurs through two channels, one from $S_n \rightarrow {}^1(T_1 T_1)$ occurring in sub-ps timescale and the other through a thermally activated ($\triangle E$) first excited singlet exciton fission $S_1 + \triangle E \rightarrow {}^1(T_1 T_1) \rightarrow 2T_1$ occurring on 40 ps timescale. The two coupled triplet excitons in the ME (or optically dark) state then diffuse apart resulting in two triplet excitons localized on individual molecules. Then the observed ESA signal refers to the $T_n \leftarrow T_1$ transition. Stimulated emission (SE) occurred from the vibrationally relaxed first excited state, here thought to be the low energy Davydov state, on 8 ps timescale.
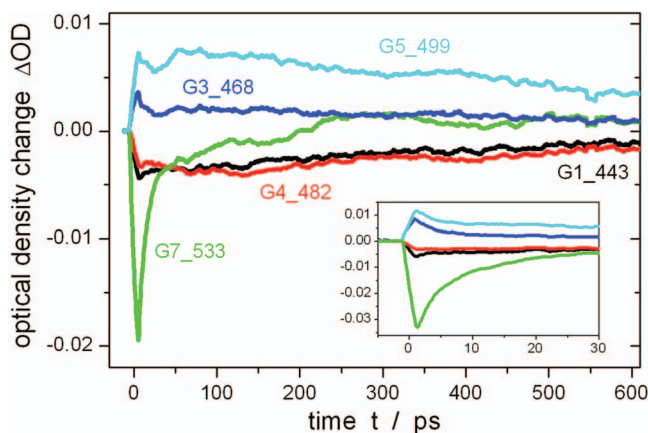

FIG. 12. The TA kinetic decay traces from the 200 nm thick crystal. The traces obtained at 443 nm, 468 nm, 482 nm, 499 nm, and 533 nm representing centers of Gaussians G1, G3, G4, G5, and G7, respectively, are displayed. The ESA (G3 and G5) and GSB (G1 and G4) signal traces were long living. The SE (G7) signal trace displayed an initial fast decay (10 ps) followed by a slow one that lasted for about 200 ps. The inset shows the initial dynamics within the first 30 ps after excitation. These signals are generated rapidly (sub-ps) soon after excitation.
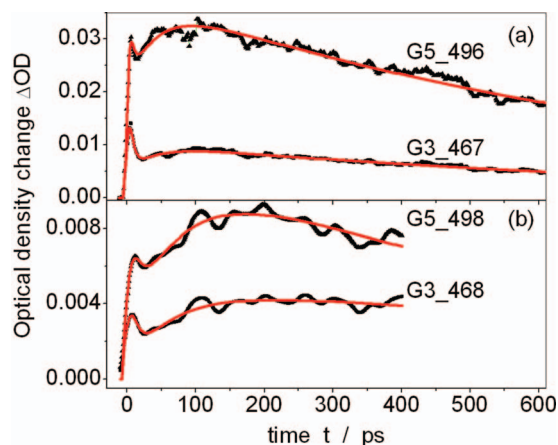
FIG. 13. The TA kinetic traces obtained from the 300 nm thick crystal excited with pump pulses centered at (a) 387 nm and (b) 530 nm both probed with white light continuum polarized $\parallel b$ axis of the crystal unit cell's (ab) facet. The ESA signals at 468 nm and at 498 nm for both excitations displayed similar initial (τ_1) and final (τ_3) decay dynamics as those of the 200 nm thick crystal. The subsequent rise (τ_2) was however different in the 530 nm excited crystal.

TABLE IV. Thermally assisted singlet fission time constant τ_2 and ratio between direct and thermally assisted fission for pump photon energies of 3.21 eV and 2.34 eV. Data are taken from analytical fits of ESA signals ascribed to $T_n \leftarrow T_1$ transitions at 498 nm and 468 nm in Figure 13.

Excitation	3.21 eV, 387 nm		2.34 eV, 530 nm	
τ_2 (thermal fission)	40 ps		80 ps	
ESA (nm)	499 nm	468 nm	498 nm	468 nm
Direct:thermal	2	1	1.8	1

attributed to a superradiant $S_1 \rightarrow S_0$ transition, as it was suggested by Burdett *et al.*[18] for fluences above a certain threshold. The latter component reflects the radiative decay of singlet excitons in Tc single crystals and is comparable to earlier reported 145 ± 50 ps.[32]

So far the results discussed in this work involved only 387 nm (3.21 eV) excitation which accessed S_n states and therefore the extra energy needed to overcome the activation barrier $\triangle E = 0.15$–0.24 eV[22,34,37] for SEF in Tc was readily available, at least initially. This explained the sub-ps rise in the kinetic traces associated with $T_n \leftarrow T_1$ transitions. Vibrationally hot states of S_1 with a total energy above $2E(T_1)$ undergo SEF as well.[21,34] If the excess excitation energy plays a key role in ps dynamics (i.e., optically induced SEF), then we would expect these to be sensitive to the photon energy of the exciting pulse. To ascertain this point, 30 fs long pulses centered at 530 nm (2.34 eV) are used to excite the 300 nm thick crystal. The obtained kinetic decay traces of the G3 and G5 ESA signals (at 468 nm and 498 nm) are displayed in Figure 13. The overall temporal profiles are similar for both excitation energies, in particular the short and the long time constants (τ_1 and τ_3) are unchanged. However, τ_2 of the thermally activated fission process and the ratio between the initial direct singlet exciton fission and the thermally activated process significantly differ for the two excitation photon energies: The fraction of direct singlet fission decreases at longer wavelength excitation, because the initial exciton energy is lower. At the same time thermally activated singlet fission (τ_2) slows down from 40 ps to 80 ps with reduction of the excitation energy, presumable again due to less excess energy for fission after vibrational relaxation within the excited singlet manifold, see Table IV.

Figure 14 displays TA spectral traces obtained with 387 nm excitation and probed with beams polarized $\perp b$ axis of the (ab) crystal face. Thus the probe interrogates the high energy Davydov component whose transition dipole moment is perpendicular to the b axis. Its 0-0 vibrational band is centered at wavelength 503 nm (2.47 eV), close to the intermediate ME state accessible with pulses centered at wavelengths between 472 nm (2.63 eV) and 489 nm (2.54 eV).[22,34,37] It is therefore expected that a substantial fraction of singlet excitons readily undergoes SEF. Noticeably, the amplitudes of the GSB signals in the obtained TA spectral traces are larger by a factor of 4 than those obtained with $\parallel b$ probing (compare GSB signals in Figures 14 and 8). This observation supports the idea of optically induced SEF being highly probable from this state in agreement with earlier results by Vaubel and Baessler.[34] In addition, the large amplitude of the trace at 500 fs after excitation implies that fission of singlets in the high energy Davydov state occurs rapidly. Weak ESA signals are also observed at 465 nm and 491 nm showing that the dominant $T_n \leftarrow T_1$ transitions are mainly $\parallel b$ polarized.

IV. CONCLUSION

We studied photo induced dynamics of singlet and triplet excitons in optically thin tetracene single crystals using ultrafast transient absorption spectroscopy in the visible spectral range. We observe fission of fs laser excited singlet excitons fission into triplet excitons occurring on different pathways and time scales. The spectral signature of the Tc triplet in the visible spectral range was identified by systematic deconvolution of the complex transient absorption spectra. As the singlet energy in tetracene is slightly lower than twice the triplet
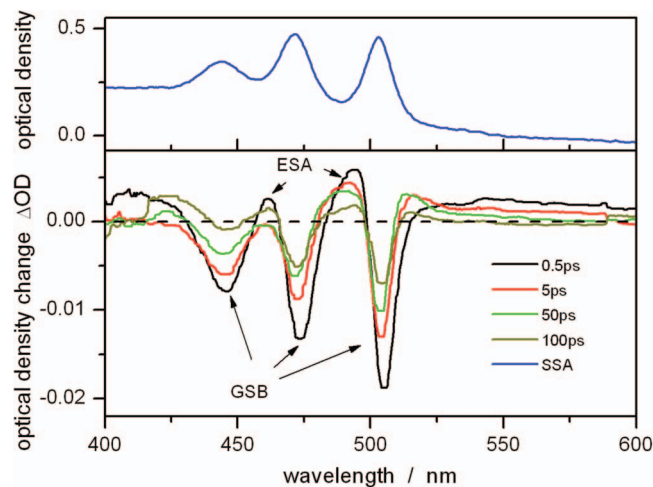

FIG. 14. The TA spectra traces obtained from the 200 nm thick crystal pumped at 387 nm and probed with WLC polarized $\perp b$ axis of the (ab) crystal face. The signal is dominated by GSB contributions which lay at exactly the same positions as those of the vibrational bands obtained from steady state absorption SSA (upper panel).

energy $E(S_1) - 2E(T_1) \approx -0.2$ eV, the additional energy must be provided by the initial laser excitation or thermal energy. We identified ultrafast fission channels from the higher Davydov state, from vibrationally excited S_1 and from higher singlet states, which are suppressed in case of laser excitation into the lowest vibration of S_1. This interpretation is supported by the fact that thermally assisted singlet exciton fission occurs faster from higher than from lower lying singlet states.

ACKNOWLEDGMENTS

[1]M. Pope, "Charge-transfer exciton state, ionic energy levels, and delayed fluorescence in anthracene," Mol. Cryst. **4**, 183–190 (1968).

[2]M. Schwoerer and H.-C. Wolf, *Organic Molecular Solids* (Wiley-VCH Verlag GmbH and Co. KGaA, Weinheim, 2007).

[3]T. Takahashi, T. Takenobu, J. Takeya, and Y. Iwasa, "Ambipolar light-emitting transistors of a tetracene single crystal," Adv. Funct. Mater. **17**, 1623–1628 (2007).

[4]C. Chien, C. Lin, M. Watanabe, Y. Lin, T. Chao, T. Chiang, X. Huang, Y. Wen, C. Tu, C. Sun, and T. Chow, "Tetracene-based field-effect transistors using solution processes," J. Mater. Chem. **22**, 13070–13075 (2012).

[5]R. de Boer, T. Klapwijk, and A. Morpurgo, "Field-effect transistors on tetracene single crystals," Appl. Phys. Lett. **83**, 4345–4347 (2003).

[6]L. Jiang, H. Dong, and W. Hu, "Organic single crystal field-effect transistors: Advances and perspectives," J. Mater. Chem. **20**, 4994–5007 (2010).

[7]Y. Xia, V. Kalihari, C. Frisbie, N. Oh, and J. Rogers, "Tetracene air-gap single-crystal field-effect transistors," Appl. Phys. Lett. **90**, 162106 (2007).

[8]C. Chu, Y. Shao, V. Shrotriya, and Y. Yang, "Efficient photovoltaic energy conversion in tetracene-C60 based heterojunctions," Appl. Phys. Lett. **86**, 243506 (2005).

[9]J.-L. Brédas, J. E. Norton, J. Cornil, and V. Coropceanu, "Molecular understanding of organic solar cells: The challenges," Acc. Chem. Res. **42**, 1691–1699 (2009).

[10]S. Tavazzi, L. Raimondo, L. Silvestri, P. Spearman, A. Camposeo, M. Polo, and D. Pisignano, "Dielectric tensor of tetracene single crystals: The effect of anisotropy on polarized absorption and emission spectra," J. Chem. Phys. **128**, 154709 (2008).

[11]S. Kena-Cohen and S. R. Forrest, "Giant Davydov splitting of the lower polariton branch in a polycrystalline tetracene microcavity," Phys. Rev. B **77**, 073205 (2008).

[12]H. Yamagata, J. Norton, E. Hontz, Y. Olivier, D. Beljonne, J. Braedas, R. Silbey, and F. Spano, "The nature of singlet excitons in oligoacene molecular crystals," J. Chem. Phys. **134**, 204703 (2011).

[13]R. He, N. Tassi, G. Blanchet, and A. Pinczuk, "Fundamental optical recombination in pentacene clusters and ultrathin films," Appl. Phys. Lett. **87**, 103107 (2005).

[14]A. Camposeo, M. Polo, S. Tavazzi, L. Silvestri, P. Spearman, R. Cingolani, and D. Pisignano, "Polarized superradiance from delocalized exciton transitions in tetracene single crystals," Phys. Rev. B **81**, 033306 (2010).

[15]M. Voigt, A. Langner, P. Schouwink, J. Lupton, R. Mahrt, and M. Sokolowski, "Picosecond time resolved photoluminescence spectroscopy of a tetracene film on highly oriented pyrolytic graphite: Dynamical relaxation, trap emission, and superradiance," J. Chem. Phys. **127**, 114705 (2007).

[16]S. Lim, T. Bjorklund, F. Spano, and C. Bardeen, "Exciton delocalization and superradiance in tetracene thin films and nanoaggregates," Phys. Rev. Lett. **92**, 107402 (2004).

[17]W. Chan, M. Ligges, and X.-Y. Zhu, "The energy barrier in singlet fission can be overcome through coherent coupling and entropic gain," Nat. Chem. **4**, 840–845 (2012).

[18]J. Burdett, A. Müller, D. Gosztola, and C. Bardeen, "Excited state dynamics in solid and monomeric tetracene: The roles of superradiance and exciton fission," J. Chem. Phys. **133**, 144506 (2010).

[19]J. Burdett, D. Gosztola, and C. Bardeen, "The dependence of singlet exciton relaxation on excitation density and temperature in polycrystalline tetracene thin films: Kinetic evidence for a dark intermediate state and implications for singlet fission," J. Chem. Phys. **135**, 214508-1–214508-10 (2011).

[20]J. Burdett and C. Bardeen, "Quantum beats in crystalline tetracene delayed fluorescence due to triplet pair coherences produced by direct singlet fission," J. Am. Chem. Soc. **134**, 8597–8607 (2012).

[21]E. Grumstrup, J. Johnson, and N. Damrauer, "Enhanced triplet formation in polycrystalline tetracene films by femtosecond optical-pulse shaping," Phys. Rev. Lett. **105**, 257403 (2010).

[22]V. Thorsmolle, R. Averitt, J. Demsar, D. Smith, S. Tretiak, R. Martin, X. Chi, B. Crone, A. Ramirez, and A. Taylor, "Morphology effectively controls singlet-triplet exciton relaxation and charge transport in organic semiconductors," Phys. Rev. Lett. **102**, 017401 (2009).

[23]H. Marciniak, B. Nickel, and S. Lochbrunner, "The ultrafast dynamics of electronic excitations in pentacene thin films," Mater. Res. Soc. Proc. **1270** (2010).

[24]O. Ostroverkhova, D. Cooke, F. Hegmann, J. Anthony, V. Podzorov, M. Gershenson, O. Jurchescu, and T. Palstra, "Ultrafast carrier dynamics in pentacene, functionalized pentacene, tetracene and rubrene single crystals," Appl. Phys. Lett. **88**, 162101 (2006).

[25]B. Gompf, D. Faltermeier, C. Redling, M. Dressel, and J. Pflaum, "Tetracene film morphology: Comparative atomic force microscopy, X-ray diffraction and ellipsometry investigations," Eur. Phys. J. E **27**, 421–424 (2008).

[26]W. Schlosser and R. Philpott, "Singlet excitons in crystalline naphthalene, anthracene, tetracene and pentacene," Chem. Phys. **49**, 181–199 (1980).

[27]M. Smith and J. Michl, "Singlet fission," Chem. Rev. **110**, 6891–6936 (2010).

[28]R. Groff, P. Avakian, and R. Merrifield, "Coexistence of exciton fission and fusion in Tetracene crystals," Phys. Rev. B **1**, 815–817 (1970).

[29]T. Berkelbach, M. Hybertsen, and D. Reichman, "Microscopic theory of singlet exciton fission. II. Application to pentacene dimers and the role of superexchange," J. Chem. Phys. **138**, 114103 (2013).

[30]T. Berkelbach, M. Hybertsen, and D. Reichman, "Microscopic theory of singlet exciton fission. I. General formulation," J. Chem. Phys. **138**, 114102 (2013).

[31]W. Mou, S. Hattori, P. Rajak, F. Shimojo, and A. Nakano, "Nanoscopic mechanisms of singlet fission in amorphous molecular solid," Appl. Phys. Lett. **102**, 173301 (2013).

[32]R. Alfano, S. Shapiro, and M. Pope, "Fission rate of singlet excitons in a tetracene crystal measured with picosecond laser pulses," Opt. Commun. **9**, 388–391 (1973).

[33]G. Klein, R. Voltz, and M. Schot, "On singlet exciton fission in anthracene and tetracene at 77°K," Chem. Phys. Lett. **19**, 391–394 (1973).

[34]G. Vaubel and H. Bässler, "Excitation spectrum of crystalline tetracene fluorescence: A probe for optically-induced singlet exciton fission," Mol. Cryst. Liq. Cryst. **15**, 15–25 (1971).

[35]G. Fleming, D. Miller, G. Morris, and G. Robinson, "Exciton Fission and annihilation in crystalline tetracene," Aust. J. Chem. **30**, 2353–2359 (1977).

[36]A. Müller, Y. Avlasevich, K. Müllen, and C. Bardeen, "Evidence of exciton fission and fusion in covalently linked tetracene dimer," Chem. Phys. Lett. **421**, 518–522 (2006).

[37]P. Zimmerman, F. Bell, D. Casanova, and M. Head-Gordon, "Mechanism for singlet fission in pentacene and tetracene: From single exciton to two triplets," J. Am. Chem. Soc. **133**, 19944–19952 (2011).

[38]W. Shockley and H. Queisser, "Detailed balance limit of efficiency of p-n junction solar cells," J. Appl. Phys. **32**, 510–519 (1961).

[39]I. Paci, J. Johnson, X. Chen, G. Rana, D. Popovic, D. David, A. Nozik, M. Ratner, and J. Michl, "Singlet fission for dye-sensitized solar cells: Can a suitable sensitizer be found?," J. Am. Chem. Soc. **128**, 16546–16553 (2006).

[40]M. Hanna and A. Nozi, "Solar conversion efficiency of photovoltaic and photoelectrolysis cells with carrier multiplication absorbers," J. Appl. Phys. **100**, 074510 (2006).

[41]J. Miller, "Multiple exciton generation enhances a working solar cell," Phys. Today **65**(2), 17–19 (2012).

[42] M. Wilson, A. Rao, J. Clark, R. Kumar, D. Brida, G. Cerullo, and R. Friend, "Ultrafast dynamics of exciton fission in polycrystalline pentacene," J. Am. Chem. Soc. **133**, 11830–11833 (2011).

[43] R. Laudise, C. Kloc, P. Simpkins, and T. Siegrist, "Physical vapor growth of organic semiconductors," J. Cryst. Growth **187**, 449–454 (1998).

[44] U. Megerle, I. Pugliesi, C. Schriever, C. Sailer, and E. Riedle, "Sub-50 fs broadband absorption spectroscopy with tunable excitation: Putting the analysis of ultrafast molecular dynamics on solid ground," Appl. Phys. B: Lasers Opt. **96**, 215–231 (2009).

[45] P. McCarthy and G. Blanchard, "Vibrational population relaxation of tetracene in n-Alkanes. Evidence for short-range molecular alignment," J. Phys. Chem. **99**, 17748–17753 (1995).

[46] P. Petelenz and M. Slawik, "Band structure of charge transfer excitons in crystalline tetracene," Chem. Phys. Lett. **178**, 337–340 (1991).

[47] L. van Dijk, "Exciton-polarons in self-assembling helical aggregates: Relating optical properties to supramolecular structure," Ph.D. thesis (Eindhoven University of Technology, 2010).

[48] R. Ortiz, R. Osuna, M. Delgado, J. Casado, V. Hernandez, J. Navarrete, Y. Sakamoto, and T. Suzuki, "Perfluorination of tetracene: Effects on the optical gap and electron-acceptor properties. An electrochemical, theoretical DFT, and Raman spectroscopic study," Proc. SPIE **6192**, 61922V (2006).

[49] R. Bensasson and E. Land, "Triplet-triplet extinction coefficients via energy transfer," Trans. Faraday Soc. **67**, 1904–1915 (1971).

[50] G. Fournie, F. Dupuy, M. Martinad, G. Nouchi, and J. Turlet, "Auto-association of tetracene in solution," Chem. Phys. Lett. **16**, 332–335 (1972).

[51] K. Liu, Y. Chen, H. Lin, C. Hsu, H. Chang, and I. Chen, "Dynamics of the excited states of p-terphenyl and tetracene: Solute-solvent interaction," J. Phys. Chem. C **115**, 22578–22586 (2011).

[52] W. Chan, M. Ligges, A. Jailaubekov, L. Kaake, L. Miaja-Avila, and X. Zhu, "Observing the multiexciton state in singlet fission and ensuing ultrafast multielectron transfer," Science **334**, 1541–1545 (2011).

[53] M. Wilson, A. Rao, K. Johnson, S. Gélinas, R. di Pietro, J. Clark, and R. Friend, "Temperature-independent singlet exciton fission in tetracene," J. Am. Chem. Soc. **135**, 16680–16688 (2013).